ortho-Phenylene-based macrocyclic hydrocarbons assembled using olefin metathesis

Viraj C. Kirinda[1], Briana R. Schrage[2], Christopher J. Ziegler[2], and C. Scott Hartley*,[1]

[1]Department of Chemistry & Biochemistry, Miami University, Oxford, Ohio 45056, United States

[2]Department of Chemistry, University of Akron, Akron, Ohio 44325, United States

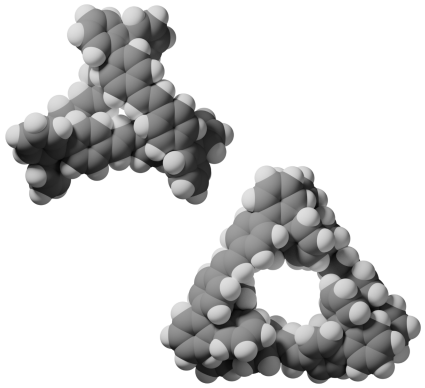

Abstract

While many foldamer systems reliably fold into well-defined secondary structures, higher order structure remains a challenge. A simple strategy for the organization of folded subunits in space is to link them together within a macrocycle. Previous work has shown that *o*-phenylenes can be co-assembled with rod-shaped linkers into twisted

macrocycles, showing an interesting synergy between folding and thermodynamically controlled macrocyclization. In these systems the foldamer units were largely decoupled from each other both conformationally and electronically. Here, we show that hydrocarbon macrocycles, with very short ethenylene linkers, can be assembled from *o*-phenylenes using olefin metathesis. Characterization by NMR spectroscopy, X-ray crystallography, and ab initio calculations shows that the products are approximately triangular [3+3] macrocycles with helical *o*-phenylene corners in a heterochiral configuration. Their photophysics are dominated by the 4,4′-diphenylstilbene moieties, the longest conjugated segments, with further conjugation broken by the twisting of the *o*-phenylenes.

Introduction

The hierarchical structure of biomacromolecules has long inspired chemists to design abiotic foldamers.[1–5] In these systems, secondary structure, especially the helix, is now fairly well represented. Higher-order structure remains rare, especially in non-peptidic foldamers, but a handful of examples have now been reported.[6–8] Simplistically, the goal is molecular architectures that place folded subunits into well-defined positions. A minimal approach to this challenge is the incorporation of foldamer moieties within conformationally restricted macrocycles.[9–11] To synthesize these targets, folding can be combined with thermodynamically controlled self-assembly, raising questions about how the two concepts together can yield products with emergent structural complexity. For helical foldamers, the products will be twisted macrocycles that combine the features of globally folded macrocycles[12–18] with those with conformationally rigid axially chiral subunits.[19–26]

Our work has focused on the *ortho*-phenylenes, an simple class of aromatic foldamers.[27] They are well-suited to the study of folding combined with self-assembly because of their straightforward conformational behavior, and because of the predictable dependence of their NMR spectra on their geometries, which allows solution-phase folding states to be

deduced and quantified. We have previously shown that amine-functionalized *o*-phenylenes can be co-assembled with aldehyde-functionalized rod-shaped linkers.[9–11] In these systems, the combination of assembly and folding yields new behavior: for example, because only certain *o*-phenylene conformers will fit within a macrocycle of a particular size, the process of macrocyclization can distort them into folds that are not observed for the unconstrained acyclic oligomers.

In this previous work, assembly occurred very effectively, but the *o*-phenylenes were conformationally and electronically decoupled from each other by their linkers. Questions remain about the tolerance of self-assembly to short restrictive linkers and the possibility of electronic coupling between the *o*-phenylenes. Here, we report the synthesis and characterization of the unsubstituted *ortho*-phenylene macrocycles $\mathbf{(oP^4)_3}$ and $\mathbf{(oP^6)_3}$, shown in Scheme 1. The macrocycles were assembled using ring closing metathesis (RCM), a well-known and efficient method for the synthesis of macrocycles[28–32] and cages.[34] These conjugated hydrocarbon macrocycles are reminiscent of other systems with Möbius π systems,[23] including an example prepared by alkyne metathesis,[36] which can lead to antiaromaticity, although the π systems of the two macrocycles reported here, despite their twisted geometries, are formally continuous.

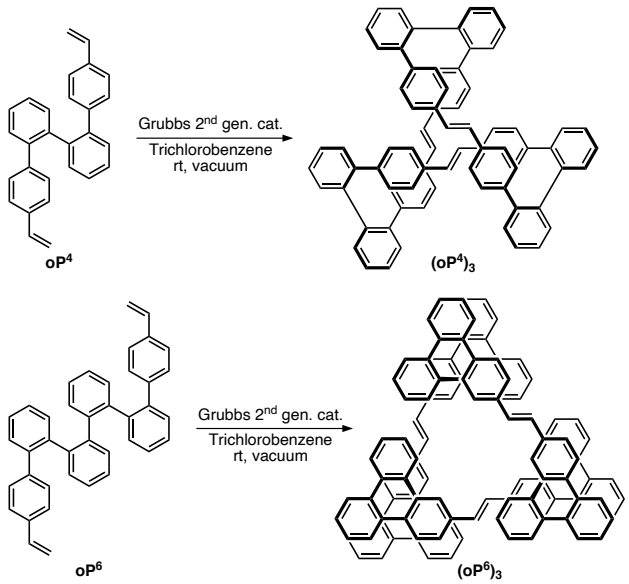

Scheme 1: Assembly of macrocycles $\mathbf{(oP^4)_3}$ and $\mathbf{(oP^6)_3}$.

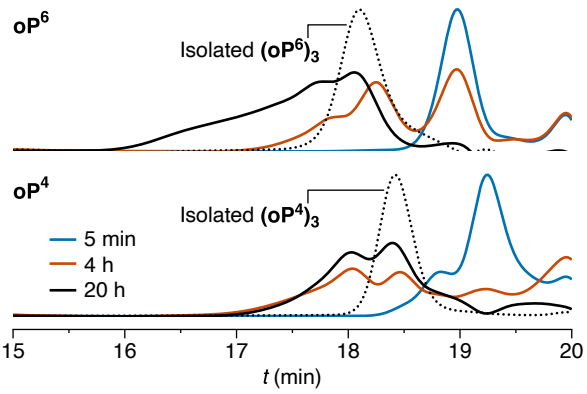

Figure 1: Monitoring of the macrocyclization of **oP^4** and **oP^6**.

Results and discussion

Synthesis

The macrocycles were synthesized from vinyl-substituted *ortho*-phenylene precursors **oP^4** and **oP^6**, whose synthesis is described in the Supporting Information. As shown in Scheme 1, these precursors (5 mM) were subjected to macrocyclization by olefin metathesis using the second-generation Grubbs catalyst in 1,2,4-trichlorobenzene at room temperature. The reactions were carried out under vacuum to remove the ethylene byproduct. Aliquots from the reaction mixtures were analyzed by analytical gel permeation chromatography (GPC). Similar product distributions, shown in Figure 1, were obtained in both cases, although there were differences in reactivity. The **oP^4** system shows peaks in the chromatograms corresponding to higher molecular weight species after only 5 min, with consumption of most of the starting **oP^4** after 4 h. While the total amount of products continues to increase, the relative proportions of higher molecular weight species do not change significantly after the 4 h mark. The reaction of **oP^6** proceeds more slowly, with significant starting material still visible for at least 8 h. In both systems, the product distribution is unchanging after 24 h, and no change was observed after adding fresh catalyst and reacting for an additional 24 h.

Macrocycles **(oP^4)$_3$** and **(oP^6)$_3$** could be isolated from the reaction mixtures by flash chromatography followed by semi-preparative GPC in 25% and 27% yields, respectively (GPC

traces in Figure 1). In both cases, mass spectrometry confirmed that the major products were the 3+3 macrocycles. Analysis of fractions corresponding to higher molecular weight species indicated the presence of higher macrocycles, although given the breadth of the peaks it is very likely that acyclic oligomers were also present.[37]

As judged by the GPC monitoring experiments, the self-assembly of these macrocycles is much less effective than that of comparable imine-based macrocycles with long linking groups, which typically give product distributions dominated by [3+3] macrocycles.[9,11] This is not so surprising given the very short ethenylene linkers of the olefin systems. Increased steric congestion could lead to either kinetic trapping or less-efficient self-assembly because of strain. Experiments where the isolated macrocycles were treated with Grubbs catalyst, to confirm (or refute) that the product distributions in Figure 1 are at equilibrium, were unfortunately inconclusive.[38]

Structural analysis of $(\mathbf{oP^4})_3$

The structures of the macrocycles can be understood in the context of the acyclic *o*-phenylenes. As shown in Figure 2, an *o*-phenylene tetramer will rapidly interconvert, via rotation about the central biaryl bond, between a "closed" conformer "A", which is stabilized by a single aromatic stacking interaction, and an extended "open" conformer "B". In chloroform, aromatic stacking is not strong enough to completely bias the system toward the folded state. The fit of an *o*-phenylene within a quasi-triangular [3+3] macrocycle can be quantified through the bite angle (β) made by the terminal positions of the oligomer (i.e., the points of attachment of the vinyl groups in $\mathbf{oP^4}$). In the A state $\beta \approx 70°$, whereas in the B state $\beta \approx 120°$ for an *o*-phenylene tetramer. Thus, as we have previously shown, only the A state fits within a triangular macrocycle (which requires $\beta \approx 60°$) and macrocyclization induces folding.[9] For $\mathbf{(oP^4)_3}$, we therefore expect a roughly triangular macrocycle with three twisted *o*-phenylene corners. This can exist, in principle, in either homochiral (*PPP* or *MMM*) or heterochiral (*PPM* or *MPP*) configurations.

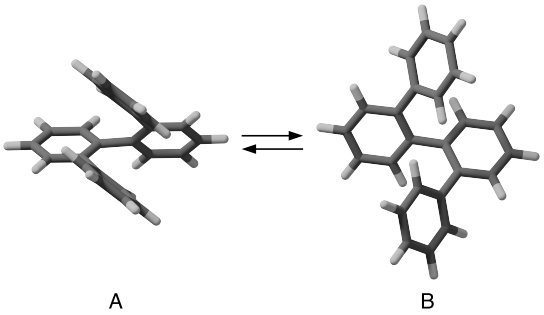

Figure 2: Conformers of tetra(*o*-phenylene). The enantiomers of these conformers will of course also be present and equally populated.

Like other *o*-phenylenes, considerable structural information can be obtained through analysis of the NMR spectra of the macrocycles, particularly when compared to acyclic analogues (i.e., **oP^4** and **oP^6**).[9,11,27] The spectrum of precursor **oP^4**, shown in Figure 3a, is a good match to that of the parent tetra(*o*-phenylene),[39] confirming that it does behave according to Figure 2, with rapid exchange on the NMR time scale. In contrast, the spectrum of cyclized **(oP^4)$_3$** is complex. Through COSY, HSQC, HMBC, and NOESY/EXSY experiments, it was possible to fully assign the spectrum (Figure 3 and Supporting Information). All of the proton signals in the spectrum are split into three (e.g., protons 1a, 1′a, 1″a), indicating that **(oP^4)$_3$** has only twofold symmetry in solution. We therefore conclude that it adopts the heterochiral C_2-symmetric geometry, and not the higher-symmetry homochiral, D_3-symmetric configuration. Comparing analogous protons between macrocyclic **(oP^4)$_3$** and acyclic **oP^4**, there are significant differences in chemical shifts (indicated in Figure 3), suggesting a change in conformational distribution for the *o*-phenylene moieties. In particular, the upfield shifts of protons 1a and downfield shifts of protons 2e indicate that, in the macrocycle, the *o*-phenylenes favor the compact A conformer as the nuclei move into and away from the shielding zones of nearby aromatic rings, respectively.[9]

We were able to grow X-ray-quality crystals of both **(oP^4)$_3$**, with the structure shown in Figure 3b, and **oP^4** (Supporting Information). The crystal structure confirms the heterochiral configuration deduced from the ^{1}H NMR analysis of the bulk solution; a freshly dissolved crystal shows an identical spectrum. Comparison of the two structures shows that the

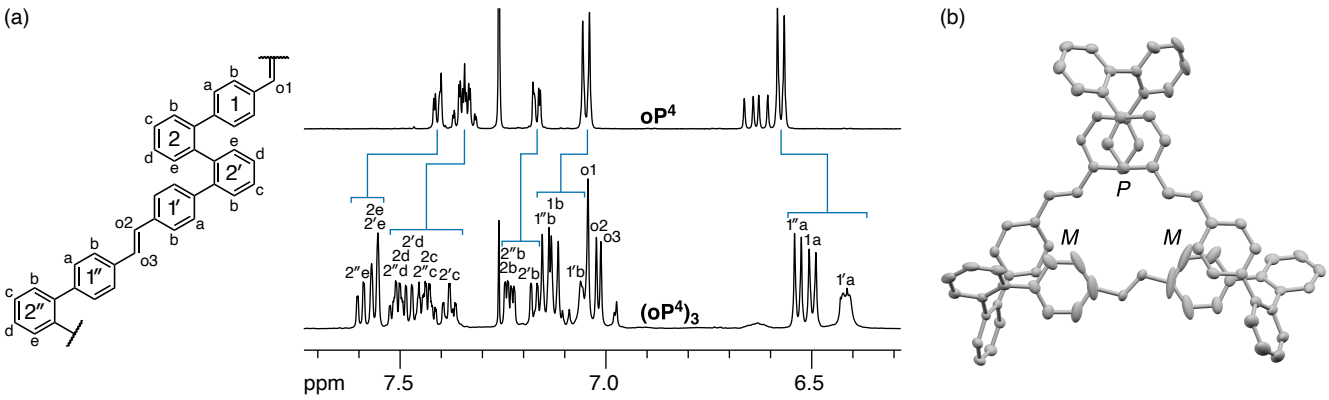

Figure 3: Characterization of $\mathbf{(oP^4)_3}$ by (a) NMR spectroscopy ($\mathbf{oP^4}$ top and $\mathbf{(oP^4)_3}$ bottom, $CDCl_3$, 500 MHz, rt) and (b) X-ray crystallography.

o-phenylenes are more tightly folded in the macrocycle, with a mean centroid-to-centroid distance between the terminal rings (1, 1′, 1″) of 3.67 Å in $\mathbf{(oP^4)_3}$, compared to 4.25 Å in $\mathbf{oP^4}$. The central dihedral angle in the *o*-phenylenes is correspondingly reduced to 60° from 62°. This compression of the *o*-phenylene moieties, and the corresponding strain, may at least partly explain the modest efficiency of self-assembly of $\mathbf{(oP^4)_3}$ compared to systems with longer, more flexible linkers.[9]

DFT geometry optimizations at the PCM($CHCl_3$)/B97-D/cc-pVDZ level were performed to further understand the conformational preferences of $\mathbf{(oP^4)_3}$. Both heterochiral and homochiral configurations and all four possible orientations of the *trans*-ethenylene groups were explicitly considered (see Supporting Information). Consistent with the NMR and crystallography results, the most-stable heterochiral conformation is predicted to be preferred over the best homochiral conformation by 4.0 kcal/mol. As was observed in the crystal structures, the DFT calculations predict that the *o*-phenylene moieties are compressed on macrocyclization. However, the effect is much smaller in the calculations (roughly 0.1 Å computationally vs 0.6 Å by crystallography). The difference is in the geometry of $\mathbf{oP^4}$, where the centroid-to-centroid distance between terminal rings is underestimated (3.67 Å vs 4.25 Å).

The conformational dynamics of the $\mathbf{(oP^4)_3}$ system were briefly explored by variable-

temperature (VT) ^{1}H NMR spectroscopy, with the spectra shown in the Supporting Information. As the temperature was decreased from room temperature to 233 K ($CDCl_3$), the internal protons of the *o*-phenylenes (rings 2, Figure 3a) did not show significant chemical shift or peak shape changes. In contrast, the signals for the terminal ring protons (rings 1) broadened. This suggests that rotation about the terminal biaryl bonds slows, as has been observed for some acyclic *o*-phenylenes with stronger aromatic stacking interactions.[40] Interestingly, the effect is more significant for the protons on rings 1 and 1′ (i.e., the *o*-phenylenes with the predominant twist senses). There is relatively little effect as the temperature is increased to 347 K, although there is some sharpening of the signal for proton 1′a, suggesting that its broadened appearance at room temperature results from conformational exchange at an intermediate rate.

Structural analysis of $(\mathbf{oP^6})_3$

The conformational behavior of *o*-phenylene hexamers is much more complex than that of tetramers. As shown in Figure 4, hexa(*o*-phenylene) can fold into a helix stabilized by three aromatic stacking interactions, called the "AAA" conformer.[40] The next most stable conformer is the "AAB" state, which differs in rotation about one of the key biaryl bonds, resulting in the loss of a single stacking interaction. Unlike *o*-phenylene tetramers, interconversion between these more sterically congested conformers is typically slow on the NMR time scale (but fast on the lab time scale). Like the tetramers, the bite angle, and thus the fit within a macrocycle of a given size, is dependent on the conformation, with only the well-folded AAA state compatible with a [3+3] macrocycle ($\beta \approx 68°$).

We were, unfortunately, unable to grow crystals of $\mathbf{(oP^6)_3}$ suitable for X-ray diffraction, despite many attempts. However, analysis of its NMR spectra and computational optimization provide insight into its structure. For reference, the NMR spectrum of the acyclic $\mathbf{oP^6}$ is shown in Figure 5a (top). At room temperature, its spectrum is a combination of sharp

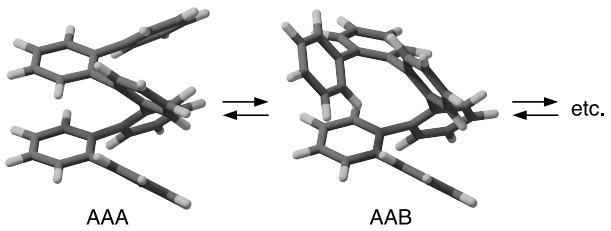

Figure 4: Conformations of hexa(*o*-phenylene).

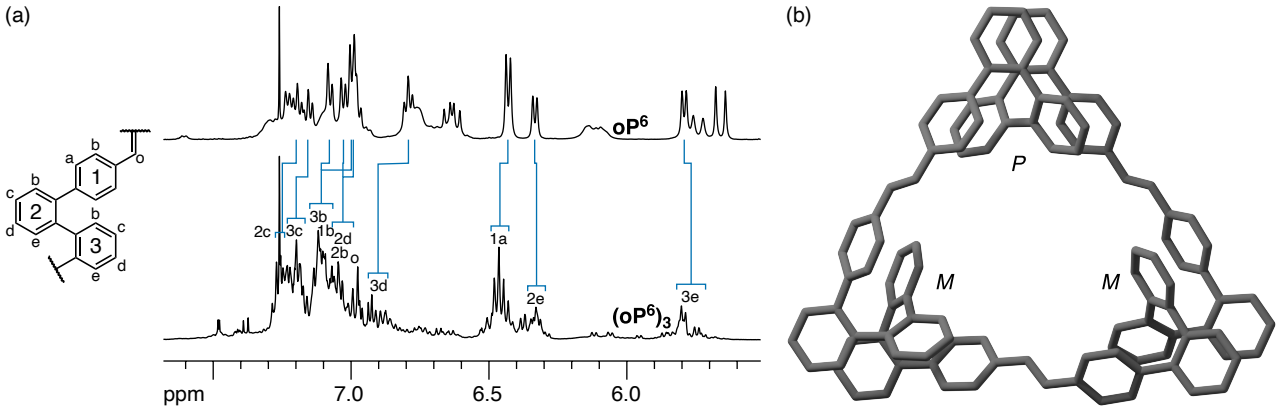

Figure 5: (a) Characterization of $\mathbf{(oP^6)_3}$ by ^{1}H NMR spectroscopy ($\mathbf{oP^6}$ top and $\mathbf{(oP^6)_3}$ bottom, $CDCl_3$, 500 MHz, rt). (b) Most-stable conformer of $\mathbf{(oP^6)_3}$, as determined by DFT optimization at the PCM($CHCl_3$)/B97-D/cc-pVDZ level.

signals associated with the perfectly folded (helical) conformation and smaller broad peaks corresponding to misfolded states, as verified by EXSY spectroscopy. As is typical for *o*-phenylenes, its ^{1}H signals could be assigned through COSY, HSQC, and HMBC spectroscopy; the assigned chemical shifts of the major conformer (see Supporting Information) are a good match to those of the parent hexa(*o*-phenylene).[39] By analogy, we conclude that $\mathbf{oP^6}$ is predominantly well-folded into the AAA state.

The ^{1}H NMR spectrum of $\mathbf{(oP^6)_3}$, shown in Figure 5a (bottom), is significantly more complex than that of the smaller $\mathbf{(oP^4)_3}$. The spectrum shows minor signals corresponding to misfolded *o*-phenylenes, as expected.[11] The assignment of these signals to misfolded conformations, as opposed to impurities, is confirmed by EXSY spectroscopy, which shows exchange peaks with signals in the major conformers, and VT NMR (see Supporting Information). As before, the chemical shifts of the major conformation were assigned using standard 2D

NMR spectra. Unfortunately, while it is clear that there are multiple symmetry-inequivalent protons in the predominant geometry, it was not possible to distinguish specific inequivalent *o*-phenylene moieties. Nevertheless, we can draw several conclusions on the basis of the spectra. First, since separate signals can be identified for many of the protons, it is clear that a D_3-symmetric homochiral conformer does not predominate. Second, since the signals for each proton do tend to be clustered together within roughly 0.1 ppm, the *o*-phenylenes must favor a single twofold-symmetric geometry as opposed to a mixture of distinct folding states. Third, the chemical shift differences for analogous protons between $\mathbf{(oP^6)_3}$ and $\mathbf{oP^6}$ are small (<0.2 ppm); confirming that the *o*-phenylenes remain similarly folded (were that not the case, many proton signals would shift by >1 ppm[11]).

At elevated temperatures (343 K), the ^{1}H NMR signals of $\mathbf{(oP^6)_3}$ broaden and coalesce, indicating significant conformational flexibility. Relatively little change in the spectrum is observed as the temperature is decreased, consistent with the oligomers already being in a slow regime for conformational exchange at room temperature.

Candidate geometries of $\mathbf{(oP^6)_3}$ were optimized at the PCM($CHCl_3$)/B97-D/cc-pVDZ level. As for $\mathbf{(oP^4)_3}$, heterochiral configurations of the macrocycle are predicted to be significantly more stable than homochiral configurations, by at least 3.8 kcal/mol. The most stable geometry is shown in Figure 5b. The *o*-phenylenes are well-accommodated by the macrocycle structure, with biaryl dihedrals along the *o*-phenylene backbone of approximately 53°, a close match to those of the parent hexa(*o*-phenylene) optimized at the same level of theory (also 53°).[11]

Photophysics

UV–vis and fluorescence spectra of $\mathbf{(oP^4)_3}$ and $\mathbf{(oP^6)_3}$ are shown in Figure 6. In principle, these macrocycles are fully conjugated around their peripheries, with 42 and 54 electrons in the shortest conjugated paths around the rings. They are therefore both formally aromatic.

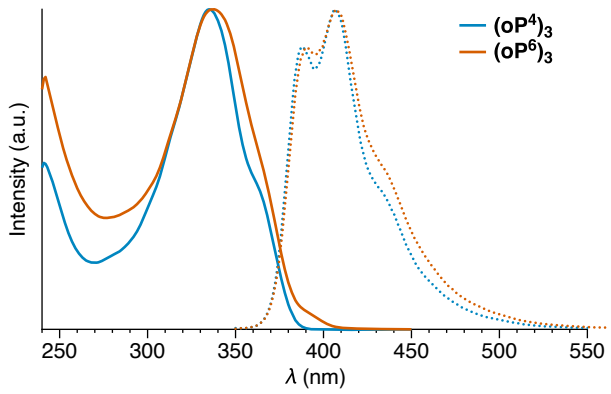

Figure 6: UV–vis (solid lines) and fluorescence (dotted lines) spectra of $\mathbf{(oP^4)_3}$ and $\mathbf{(oP^6)_3}$ in chloroform.

However, folded *ortho*-phenylenes lack extended π-conjugation.[41,42] Consequently, the two macrocycles show similar photophysical properties despite the different oligomer lengths. Their UV–vis spectra are similar in shape, with maximum absorption wavelengths (λ_{max}) of 335 nm and 337 nm for $\mathbf{(oP^4)_3}$ and $\mathbf{(oP^6)_3}$, respectively. These spectra are a close match to that of (*E*)-4,4′-diphenylstilbene (λ_{max} = 342 nm),[43,44] which represents a single side of each macrocycle excluding conjugation through the *o*-phenylene moieties. Curiously, despite the structural and spectral similarities, the macrocycles show significantly different absorptivities, with that of $\mathbf{(oP^6)_3}$ approximately double that of $\mathbf{(oP^4)_3}$ ($(7.9 \pm 0.6) \times 10^4$ M^{-1} vs $(3.8 \pm 0.3) \times 10^4$ M^{-1}). The fluorescence spectra (Figure 6) are likewise similar and a good match to that of 4,4′-diphenylstilbene.[44] Both macrocycles are strongly fluorescent, with quantum yields of 0.88 and 0.81 for $\mathbf{(oP^4)_3}$ and $\mathbf{(oP^6)_3}$, respectively (which are indistinguishable within experimental uncertainty). Fluorescence lifetimes were determined by time-correlated single photon counting. Both compounds gave good monoexponential fits with lifetimes of 1.4 ns and 1.1 ns for $\mathbf{(oP^4)_3}$ and $\mathbf{(oP^6)_3}$.

Conclusions

Twisted macrocycles $\mathbf{(oP^4)_3}$ and $\mathbf{(oP^6)_3}$ have been synthesized and characterized. Assembly by olefin metathesis is reasonably efficient, considering their sterically congested structures and

the strain introduced on macrocyclization by the very short linkers. Characterization by NMR spectroscopy and X-ray crystallography shows that macrocycle $\mathbf{(oP^4)_3}$ favors a C_2-symmetric, heterochiral geometry in both solution and the solid-state. DFT optimization confirms that this is indeed the most stable conformer for this system. Both X-ray crystallography and the DFT calculations show that the *o*-phenylene moieties are compressed in $\mathbf{(oP^4)_3}$, indicating strain that may explain the relatively low yield. Similar behavior is observed for $\mathbf{(oP^6)_3}$. The macrocycle favors a heterochiral configuration of well-folded *o*-phenylene moieties, although misfolded states are observed by NMR spectroscopy. The photophysical properties of the two systems are very similar, with nearly identical absorbance and fluorescence spectra that can be assigned to 4,4′-diphenylstilbene chromophores, indicating that the twisted *o*-phenylenes break conjugation.

Acknowledgements

CSH and VCK (synthesis, NMR spectroscopy, computational chemistry, photophysics) thank the National Science Foundation (CHE-1608213 and CHE-1904236) for support of this work and the Volwiler Distinguished Research Professorship. CJZ and BRS (crystallography) would like to acknowledge the University of Akron for support of this research.

References

(1) Gellman, S. H. Foldamers: a manifesto. *Acc. Chem. Res.* **1998**, *31*, 173–180.

(2) Guichard, G.; Huc, I. Synthetic foldamers. *Chem. Commun.* **2011**, *47*, 5933–5941.

(3) Hill, D. J.; Mio, M. J.; Prince, R. B.; Hughes, T. S.; Moore, J. S. A field guide to foldamers. *Chem. Rev.* **2001**, *101*, 3893–4011.

(4) Saraogi, I.; Hamilton, A. D. Recent advances in the development of aryl-based foldamers. *Chem. Soc. Rev.* **2009**, *38*, 1726–1743.

(5) Le Bailly, B. A. F.; Clayden, J. Dynamic foldamer chemistry. *Chem. Commun.* **2016**, *52*, 4852–4863.

(6) Mazzier, D.; De, S.; Wicher, B.; Maurizot, V.; Huc, I. Parallel homochiral and antiparallel heterochiral hydrogen-bonding interfaces in multi-helical abiotic foldamers. *Angew. Chem., Int. Ed.* **2020**, *59*, 1606–1610.

(7) Mazzier, D.; De, S.; Wicher, B.; Maurizot, V.; Huc, I. Interplay of secondary and tertiary folding in abiotic foldamers. *Chem. Sci.* **2019**, *10*, 6984–6991.

(8) De, S.; Chi, B.; Granier, T.; Qi, T.; Maurizot, V.; Huc, I. Designing cooperatively folded abiotic uni- and multimolecular helix bundles. *Nat. Chem.* **2018**, *10*, 51–57.

(9) Kinney, Z. J.; Hartley, C. S. Twisted macrocycles with folded *ortho*-phenylene subunits. *J. Am. Chem. Soc.* **2017**, *139*, 4821–4827.

(10) Kinney, Z. J.; Hartley, C. S. Linker-directed assembly of twisted *ortho*-phenylene-based macrocycles. *Org. Lett.* **2018**, *20*, 3327–3331.

(11) Kinney, Z. J.; Kirinda, V. C.; Hartley, C. S. Macrocycles of higher ortho-phenylenes: assembly and folding. *Chem. Sci.* **2019**, *10*, 9057–9068.

(12) Zhang, Z.; Cha, W.-Y.; Williams, N. J.; Rush, E. L.; Ishida, M.; Lynch, V. M.; Kim, D.; Sessler, J. L. Cyclo[6]pyridine[6]pyrrole: A dynamic, twisted macrocycle with no meso bridges. *J. Am. Chem. Soc.* **2014**, *136*, 7591–7594.

(13) Liu, B.; Pappas, C. G.; Zangrando, E.; Demitri, N.; Chmielewski, P. J.; Otto, S. Complex molecules that fold like proteins can emerge spontaneously. *J. Am. Chem. Soc.* **2019**, *141*, 1685–1689.

(14) Reiné, P.; Justicia, J.; Morcillo, S. P.; Abbate, S.; Vaz, B.; Ribagorda, M.; Orte, Á.; Álvarez de Cienfuegos, L.; Longhi, G.; Campaña, A. G.; Miguel, D.; Cuerva, J. M. Pyrene-containing *ortho*-oligo(phenylene)ethynylene foldamer as a ratiometric probe based on circularly polarized luminescence. *J. Org. Chem.* **2018**, *83*, 4455–4463.

(15) Urushibara, K.; Ferrand, Y.; Liu, Z.; Masu, H.; Pophristic, V.; Tanatani, A.; Huc, I. Frustrated helicity: joining the diverging ends of a stable aromatic amide helix to form a fluxional macrocycle. *Angew. Chem., Int. Ed.* **2018**, *57*, 7888–7892.

(16) Katoono, R.; Tanaka, Y.; Fujiwara, K.; Suzuki, T. A foldable cyclic oligomer: chiroptical modulation through molecular folding upon complexation and a change in temperature. *J. Org. Chem.* **2014**, *79*, 10218–10225.

(17) Chen, F.; Tanaka, T.; Hong, Y.; Kim, W.; Kim, D.; Osuka, A. *ortho*-Phenylene-bridged cyclic oligopyrroles: Conformational flexibilities and optical properties. *Chem.—Eur. J.* **2016**, *22*, 10597–10606.

(18) Hjelmgaard, T.; Nauton, L.; De Riccardis, F.; Jouffret, L.; Faure, S. Topologically diverse shapes accessible by modular design of arylopeptoid macrocycles. *Org. Lett.* **2018**, *20*, 268–271.

(19) Caricato, M.; González, S. D.; Arandia Ariño, I.; Pasini, D. Homochiral BINOL-based macrocycles with π-electron-rich, electron-withdrawing or extended spacing units as receptors for C_{60}. *Beilstein J. Org. Chem.* **2014**, *10*, 1308–1316.

(20) Widhalm, M.; Wimmer, P.; Klintschar, G. Macrocyclic diphosphine ligands in asymmetric carbon-carbon bond-forming reactions. *J. Organomet. Chem.* **1996**, *523*, 167–178.

(21) Castro-Fernández, S.; Cid, M. M.; López, C. S.; Alonso-Gómez, J. L. Opening access to new chiral macrocycles: from allenes to spiranes. *J. Phys. Chem. A* **2015**, *119*, 1747–1753.

(22) Rivera-Fuentes, P.; Diederich, F. Allenes in molecular materials. *Angew. Chem., Int. Ed.* **2012**, *51*, 2818–2828.

(23) Schaller, G. R.; Topić, F.; Rissanen, K.; Okamoto, Y.; Shen, J.; Herges, R. Design and synthesis of the first triply twisted Möbius annulene. *Nat. Chem.* **2014**, *6*, 608–613.

(24) Sisco, S. W.; Moore, J. S. Homochiral self-sorting of BINOL macrocycles. *Chem. Sci.* **2014**, *5*, 81–85.

(25) Malik, A. U.; Gan, F.; Shen, C.; Yu, N.; Wang, R.; Crassous, J.; Shu, M.; Qiu, H. Chiral organic cages with a triple-stranded helical structure derived from helicene. *J. Am. Chem. Soc.* **2018**, *140*, 2769–2772.

(26) Naulet, G.; Sturm, L.; Robert, A.; Dechambenoit, P.; Röhricht, F.; Herges, R.; Bock, H.; Durola, F. Cyclic tris-[5]helicenes with single and triple twisted Möbius topologies and Möbius aromaticity. *Chem. Sci.* **2018**, *9*, 8930–8936.

(27) Hartley, C. S. Folding of *ortho*-phenylenes. *Acc. Chem. Res.* **2016**, *49*, 646–654.

(28) Zhang, W.; Moore, J. S. Reaction pathways leading to arylene ethynylene macrocycles via alkyne metathesis. *J. Am. Chem. Soc.* **2005**, *127*, 11863–11870.

(29) Lee, C. W.; Grubbs, R. H. Formation of macrocycles via ring-closing olefin metathesis. *J. Org. Chem.* **2001**, *66*, 7155–7158.

(30) Bergman, Y. E.; Del Borgo, M. P.; Gopalan, R. D.; Jalal, S.; Unabia, S. E.; Ciampini, M.; Clayton, D. J.; Fletcher, J. M.; Mulder, R. J.; Wilce, J. A.; Aguilar, M.-I.; Perlmutter, P. Synthesis of stapled β^3-peptides through ring-closing metathesis. *Org. Lett.* **2009**, *11*, 4438–4440.

(31) Ogba, O. M.; Warner, N. C.; O'Leary, D. J.; Grubbs, R. H. Recent advances in ruthenium-based olefin metathesis. *Chem. Soc. Rev.* **2018**, *47*, 4510–4544.

(32) Jin, Y.; Zhang, A.; Huang, Y.; Zhang, W. Shape-persistent arylenevinylene macrocycles (AVMs) prepared via acyclic diene metathesis macrocyclization (ADMAC). *Chem. Commun.* **2010**, *46*, 8258–8260.

(34) Moneypenny II, T. P.; Walter, N. P.; Cai, Z.; Miao, Y.-R.; Gray, D. L.; Hinman, J. J.; Lee, S.; Zhang, Y.; Moore, J. S. Impact of shape persistence on the porosity of molecular cages. *J. Am. Chem. Soc.* **2017**, *139*, 3259–3264.

(36) Jiang, X.; Laffoon, S. D.; Chen, D.; Pérez-Estrada, S.; Danis, A. S.; Rodríguez-López, J.; Garcia-Garibay, M. A.; Zhu, J.; Moore, J. S. Kinetic control in the synthesis of a Möbius tris((ethynyl)[5]helicene) macrocycle using alkyne metathesis. *J. Am. Chem. Soc.* **2020**, *142*, 6493–6498.

(37) Hartley, C. S.; Elliott, E. L.; Moore, J. S. Covalent assembly of molecular ladders. *J. Am. Chem. Soc.* **2007**, *129*, 4512–4513.

(38) The macrocycles simply decomposed to lower-molecular-weight species.

(39) Mathew, S. M.; Hartley, C. S. Parent *o*-phenylene oligomers: synthesis, conformational behavior, and characterization. *Macromolecules* **2011**, *44*, 8425–8432.

(40) Mathew, S.; Crandall, L. A.; Ziegler, C. J.; Hartley, C. S. Enhanced helical folding of *ortho*-phenylenes through the control of aromatic stacking interactions. *J. Am. Chem. Soc.* **2014**, *136*, 16666–16675.

(41) Ando, S.; Ohta, E.; Kosaka, A.; Hashizume, D.; Koshino, H.; Fukushima, T.; Aida, T. Remarkable effects of terminal groups and solvents on helical folding of *o*-phenylene oligomers. *J. Am. Chem. Soc.* **2012**, *134*, 11084–11087.

(42) He, J.; Mathew, S. M.; Cornett, S. D.; Grundy, S. C.; Hartley, C. S. *ortho*-Phenylene oligomers with terminal push-pull substitution. *Org. Biomol. Chem.* **2012**, *10*, 3398–3405.

(43) Fengqiang, Z.; Motoyoshiya, J.; Nishii, Y.; Aoyama, H.; Kakehi, A.; Shiro, M. Different photochemical behavior of bis(biphenyl)ethylenes and ethenes in solution and in the solid-state: Structurally controlled Z/E-photoisomerization in the solid-state. *J. Photochem. Photobiol., A* **2006**, *184*, 44–49.

(44) Andreeshchev, E. A.; Viktorova, V. S.; Kilin, S. F.; Kushakevich, Y. P.; Rozman, I. M. Absorption and fluorescence spectra of stilbene, diphenylstilbene and styrylstilbene. *Opt. Spektrosk.* **1968**, *24*, 387–390.